Monitoring the Electronics Performance of the Ring Imaging CHerenkov Counter (RICH)

Julia Tsitron

Department of Physics and Astronomy,

Hunter College, New York, New York, 10021

(Dated: 15 August 2003)

The Ring Imaging Cherenkov Counter (RICH) is used to help identify particles produced in the interaction region of the Cornell Electron-Positron Storage Ring (CESR). Since the installation of the RICH in 1999, a number of studies into the behavior of its electronics system have been conducted. This summer, the primary focus of my research was to carry out another such investigation. This work consisted of two main parts: running various Calibration Modes on the RICH teststand as well as on the detector itself, and performing statistical analyses into the nature of noise and "flatness" in the readout electronics. The results from Small Calibration, Single Channel Calibration, and Big Calibration runs are presented, as well as plots that describe the long term behavior of noise levels and flat chips in the RICH. Finally, photon-like pulse height distributions were surveyed for each window of the RICH and these results are also included.
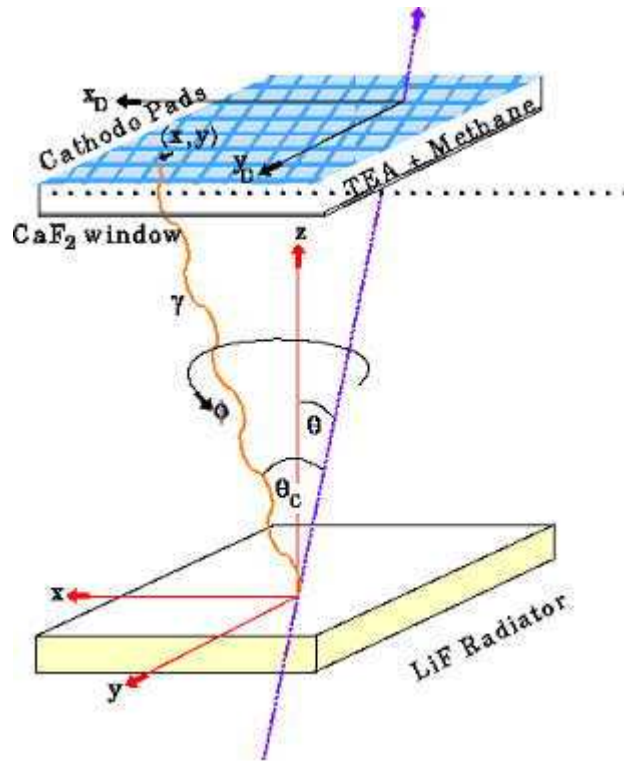
I. INTRODUCTION

FIG. 1: Diagram of the RICH detector.

The design of the RICH detector is based on a phenomenon known as the Cherenkov effect, named after the Russian scientist who studied its properties extensively in the 1930's [1]. When highly energetic particles, such as the ones created in CLEO III [2] after electron-positron collisons, travel through a medium at a velocity greater than the speed of light in that medium, Cherenkov radiation is emitted in a cone-shaped pattern around the particle's trajectory. The half-angle of the cone is given by the following formula:

$$\cos\theta = \frac{1}{n\beta} \tag{1}$$

where

$$\beta = \frac{v}{c} \tag{2}$$

and v is the speed of the particle, n is the index of refraction of the medium, and c is the speed of light in vacuum.

In the RICH detector the medium that is used to produce these Cherenkov photons is a thin radiator made of Lithium Flouride (LiF) Crystals. Once the particle and its Cherenkov cone pass through the radiator they enter an expansion volume filled with Nitrogen gas, a substance which was chosen for its minimal interaction with photons. The purpose of the expansion volume is to allow the space between individual photons and the particle itself to increase for easier detection and identification in the next stage of the process. After passing through the expansion volume, the photons enter what is essentially a photon detector consisting of the following components:: a CaF_2 window which is deposited with metallic traces kept at -1200 V, a chamber containing a mixture of Methane (CH_4) and Triethylamine (TEA), a photosensitive gas, a multi-wire proportional counter with anode wires kept at +1500 V, and a cathode grid. As the photons pass through the CaF_2 window they ionize the gas molecules in the chamber and the freed electrons which are accelerated within the electric field. Meanwhile these electrons ionize even more gas molecules and the result is an avalanche of electrons being deposited on the anode wires which are capacitively coupled to the cathode pads located at the upper end of the photon detector.

A signal from a cathode pad is then sent to be processed by the readout electronics located on the reverse side of the cathode boards. The configuration of the readout electronics is as follows: A total number of 230,400 channels need to be handled. These are divided into 30 chambers or sectors within the detector. Each chamber is subdivided into 12 readout chains which are connected via ribbon cables to the data boards (three chains per board) located in the front end crates (14-16 boards per crate.) There is a total of eight crates, and they sit outside of the detector cylinder, four on each end. A single chain consists of ten specially designed VLSI chips, called VA RICH, which were developed for the low noise/high dynamic range requirements of the RICH [3]. Each chip consists of a preamplifier, shaper and sample and hold circuits used to process the charge signals coming in from the cathode pads. Two 64-channel chips are mounted together on one hybrid circuit to form a "chip-carrier" containing 128 channels. The VA RICH outputs an analog signal which is then sent to a 12-bit differential analog to digital converter (ADC). There is one ADC for each chip-carrier so a data board contains 15 ADC's (one for each of the five chip-carriers on each of the three chains).

Because of the extensive nature and complexity of the RICH readout electronics it is necessary to continually monitor the behavior of individual components of this system. Some of the tools used this summer to conduct these studies include the following: 1.Studying pedestal plots from Small Calibration Runs in order to determine the noise levels in the

detector, and to identify chips or channels that are not functioning properly 2.Performing Single Channel Calibration (SCC) to characterize the electronic gain function of indivdual channels 3.Running "Big Cal" which is essentially SCC for each of the 230,400 channels in the RICH 4.Looking at the chamber gain of each window of the detector.

II.   SMALL CALIBRATION RUNS, "FLATNESS" AND NOISE

Small Calibration runs are just like data-taking runs except they are performed when the accelerator is off. The purpose is to measure the background or pedestal values that each channel is reading. These pedestal values are later subtracted from the ADC values that are read for an actual event during data-taking. Pedestal plots produced from Small Calibration Runs are also useful when trying to diagnose channels or chips that are malfunctioning. An example of a chip that is not working properly is a "flat chip," which can be identified visually from a pedestal plot such as the one in Fig. 2. The flat line seen in the second chip
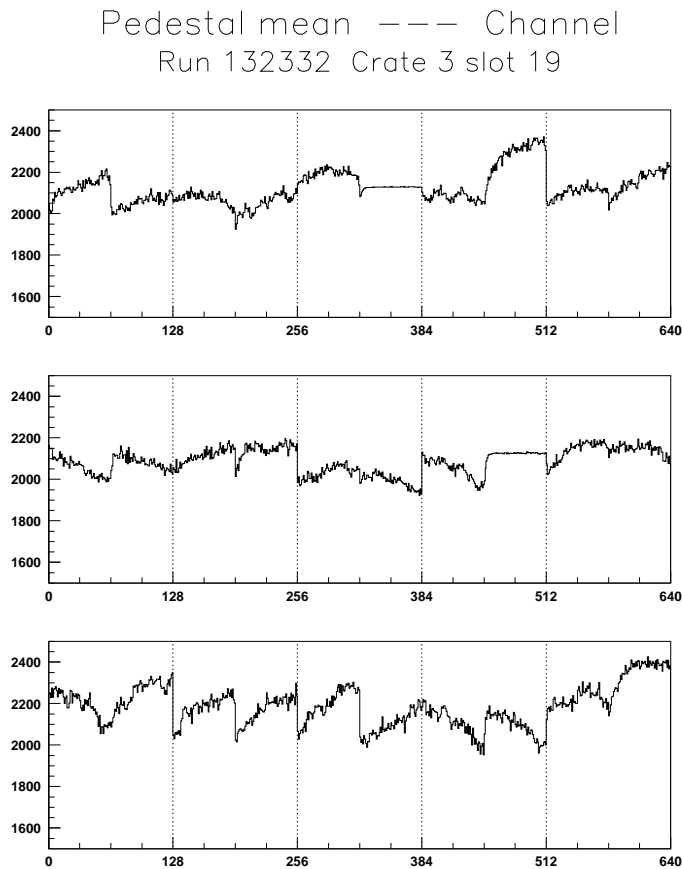

FIG. 2: This is a readout of pedestal values for three chains in the detector. The second chip of the third chip-carrier of the first chain is reading approximately the same value for each of its channels.

of the third chip-carrier of the first chain as well as in the fourth chip-carrier of the second chain shows us that each of the channels in these chips is reading approximately the same

value for each of its channels. This is an indication that the chips are not working as they should be and we are not to believe the information we read from them during an actual event. The number of flat chips has been increasing since the RICH was installed four years ago. This poses a big problem since the more flat chips there are in the detector as a whole the less useful data we have to work with. It is crucial, therefore, to find the root of the problem so that flatness can be minimized and the chips that have exhibited this condition can be brought back to working condition.

Several studies have been carried out in an attempt to find the explanation behind flatness[4]. One hypothesis is a condition called latch-up [5] which is brought on by high noise levels in the electronics. To study more closely the possible correlation between noise and flatness in the RICH I looked at Small Calibration runs for the past three years to see if the number of channels that are inherently noisy has been increasing. The plot in Fig. 3 shows the number of noisy channels versus time (or Version Number which corresponds to a point in time - Version Numbers are assigned in chronological order).
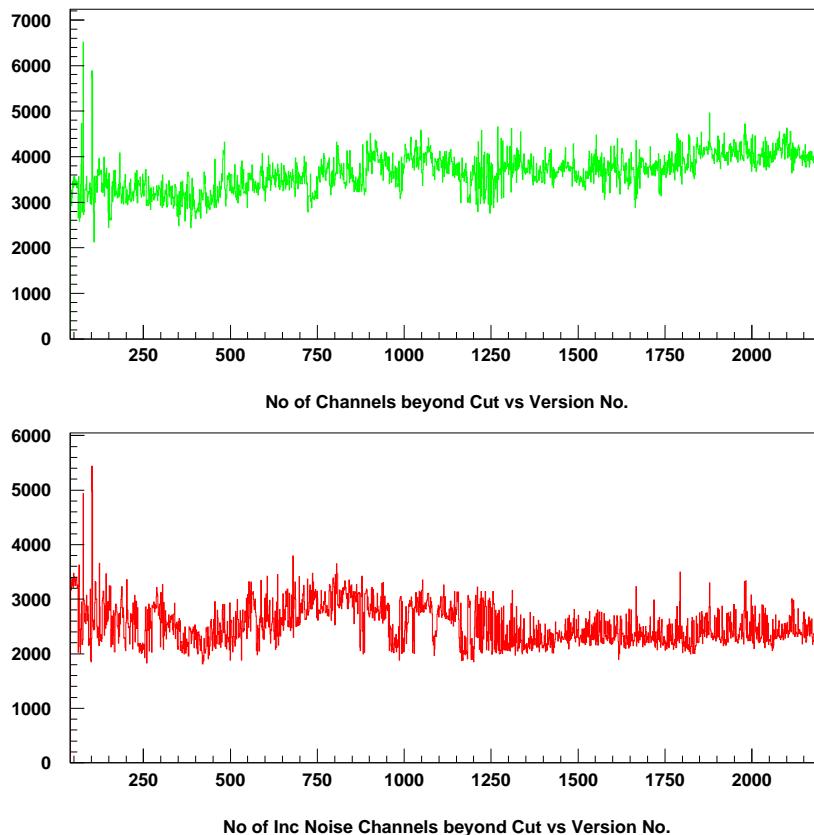

FIG. 3: The number of noisy channels over the last three years.

The top graph shows the number of "total noise" channels and the bottom graph shows the number of "incoherent noise" channels. Total noise is defined as the spread of the distribution of pedestal values for a single run. Incoherent noise is the "total noise" minus the amount by which the chip average pedestal values shift from event to event. The two graphs depicted here give us the number of noisy channels based on the following cut: If the noise distribution for a given run is like the one pictured in Fig. 4, which is very close to a

Gaussian, then a noisy channel would be found in the "tail" of the distribution (beyond the blue line).
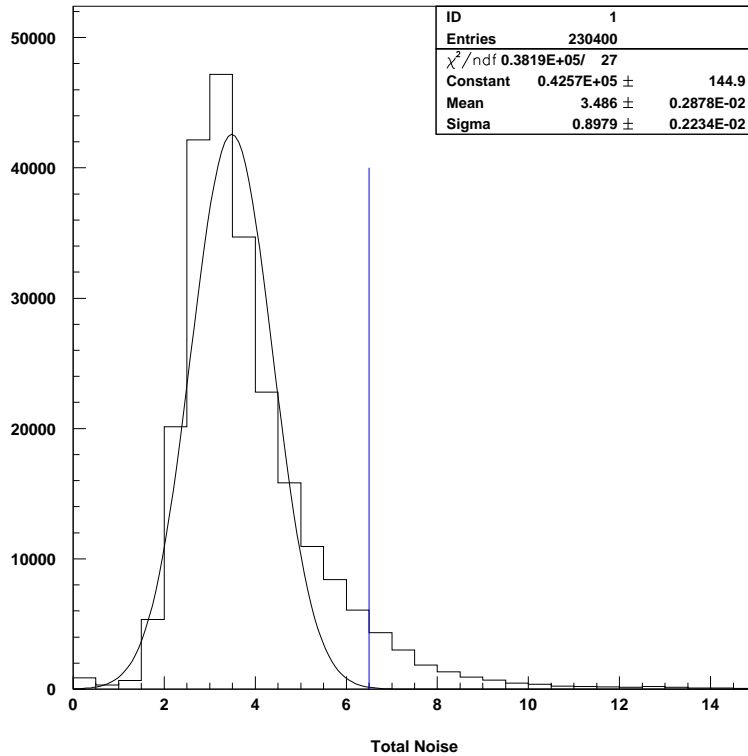

FIG. 4: This is a typical distribution of Total Noise for a Small Calibration run. Noisy channels would be those found beyond the blue cut-off line or in the "tail" of the distribution.

In order to make some sense out of the way a channel is characterized as noisy, it is important to know how the value of this "tail" or cut-off point is assigned. For the plot in Fig. 3 it was defined as the mean of the noise distribution for a given run plus three times the spread of that distribution. In other words,

$$tail = <x> + 3 * rms \tag{3}$$

where

$$rms = \sqrt{<x^2> - <x>^2} \tag{4}$$

and

$$<x> = \sum_{k=1}^{N} x_k / N \tag{5}$$

$$<x^2> = \sum_{k=1}^{N} x_k^2 / N \tag{6}$$

N is always 230,400 the total number of channels in the RICH.

This definition of the tail is only useful if the distributions of both total noise and incoherent noise do not fluctuate too much in time. I examined the behavior of the value of the cut-off point for the same Version Numbers (for the same three year period) in the plot shown in Fig. 5.
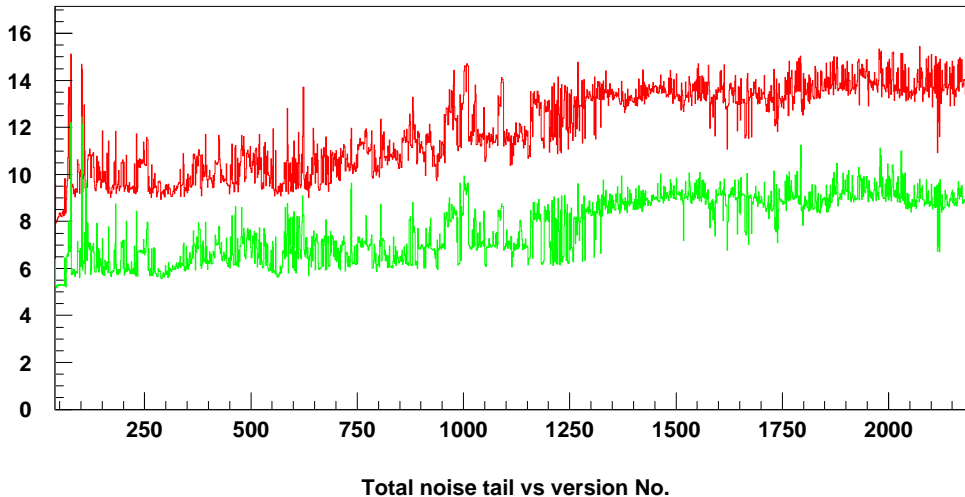
Total noise tail vs version No.

FIG. 5: The top (red) curve is the value of the tail for total noise v. time; the lower (green) line the value of the tail for incoherent noise v. time.

We see from this plot that the value of both the total noise tail as well as the incoherent noise tail is increasing with time, which is an indication that there must be some fluctuation in the distributions of noise. More specifically, based on our definition, this increase could have been caused by either of two factors: the mean value of total noise and incoherent noise is rising, or the spread of those distributions is getting bigger.

In Fig. 6 we see that the average number of total noise and incoherent noise has remained pretty stable over the last three years. The spread, however, is increasing. Therefore, our definition of the cut-off point for "noisyness" will not necessarily give us a useful measure of the number of channels that are noisy. The decision was then to redefine the cut-off point as a fixed value. The new definition meant that a channel would be classified as noisy if it measured more than 10 ADC counts for total noise, or more than 6 ADC counts for incoherent noise.

Fig. 7 is a plot of the number of noisy channels, this time based on fixed cuts. Right below it in Fig.8 we see the number of flat chips, over the same three years. The number of "total noise" channels rose from about 1.2% of the total number of channels in the RICH (230,400) to approximately 2.8%, incoherent noise channels from about 2.6% to 3.5%. The number of flat chips rose from about 2.4% of the total number of chips (3600) to 4.9%. These figures, and the visual scan of these three graphs suggests that there is indeed a correlation between flatnees and noise in the RICH detector.

III.   SINGLE CHANNEL CALIBRATION AND "BIG CAL"

Another Calibration mode that I used to study the readout electronics of the RICH was Single Channel Calibration (SCC). In SCC a charge signal is injected into the electronics where normally (in a Small Cal or data-taking run) the signal would be coming in from
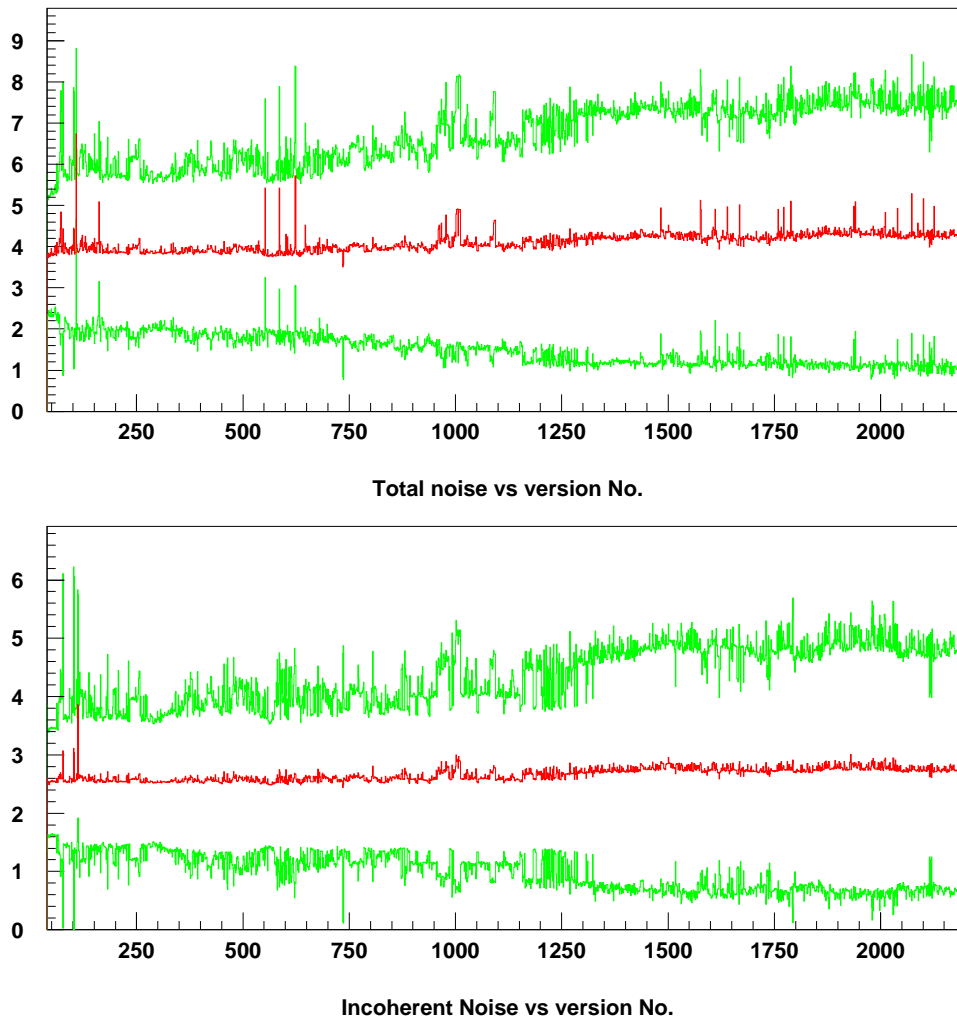
FIG. 6: This graph shows the total noise and incoherent noise over the last three years. The central (red) lines are the average values while the outer (green) lines indicate the spread of values.

the cathode pads. Then the signal is sent to be processed by the chip-carrier the way it ordinarily does, with one difference: instead of sending the pulse to each of its 128 channels, it is sent to only one channel of the chip-carrier. The VA RICH outputs an analog signal, a hold is applied at the peak, and it is finally sent to the ADC. We can then read the digital readout, the range being 0-4096 ADC counts. The idea is that since we ourselves send the pulse into the system we know the value of that signal. We also know what the ADC readout is. If we send different sized signals to a single channel and then observe the response to each of those pulses, we could characterize the electronic gain curve for that channel. This would allow us to have a better understanding of what an ADC value means in terms of what actually occured in the detector [4].

The first step was to run SCC on the RICH teststand. A pulse was sent to the 77th channel of each chip-carrier. Fig. 9 is a readout of a SCC run that was successful. Since
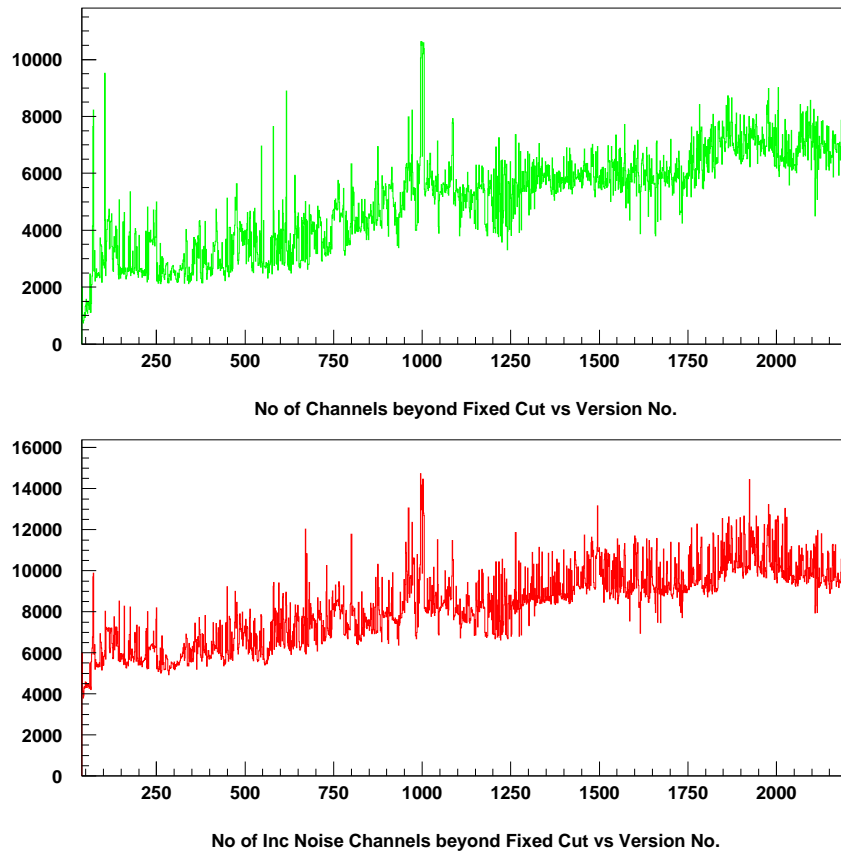
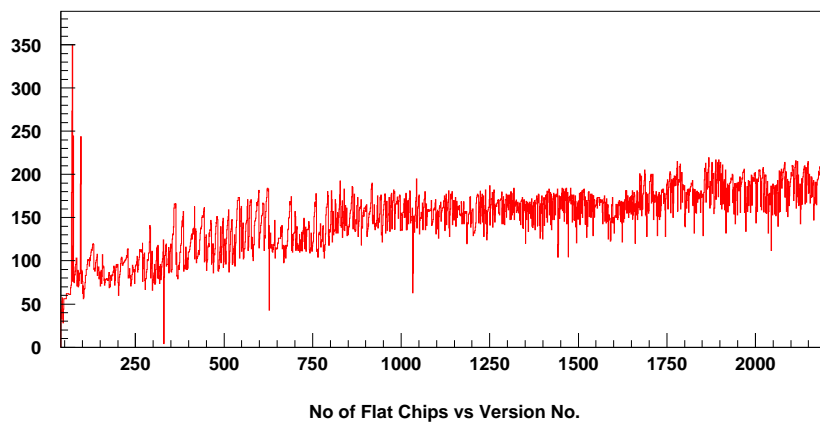FIG. 7: The number of noisy channels based on fixed cuts.

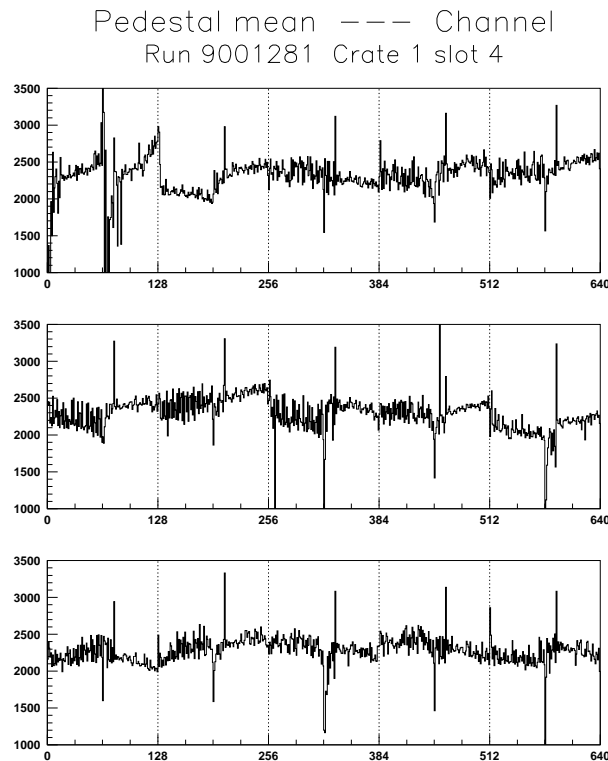FIG. 8: The number of flat chips over the same time period.

FIG. 9: This is a readout of a SCC run on the three chains of the RICH teststand. Notice the spike at the 77th channel of each chip-carrier.

we injected a signal into only one of the channels we expected to see a spike in the graph in each of the chip-carriers at the 77th channel. That was indeed the case and Fig. 10 is a close-up of the first chip-carrier of the second chain which gives us a better view of that spike. Notice also that the remaining channels are reading pedestal values just like the ones in Fig. 2. Because we injected a signal into the system, it introduced some noise into some of the neighboring channels, which explains why these pedestal curves have more of an erratic behavior than in our plot from a Small Calibration run. This is not to be confused with the inherent noise of the electronics, which was discussed in the previous section.

Once Single Channel Calibration was working we decided to move on to Big Calibration mode. "Big Cal" is Single Channel Calibration performed on each of the 230,400 channels of the RICH. This means sending nine different pulse heights into each of the 128 channels of the 1800 chip-carriers in the detector. Big Cal has never been performed before and the information to be gained from such a job would highly improve the quality of the reconstructions of charged particle tracks in the detector.

The first step was running Big Cal on the teststand. The initial plan was to perform Big Cal as a single run. This means sending a pulse into each of the 128 channels and then repeating for seven different pulse heights. This proved to be too much for the system to handle. The solution was to split up the process into several runs, however there was a concern that if there were too many steps the job would simply be too time consuming to be of any practical use. The compromise was to send one pulse to 64 channels in each
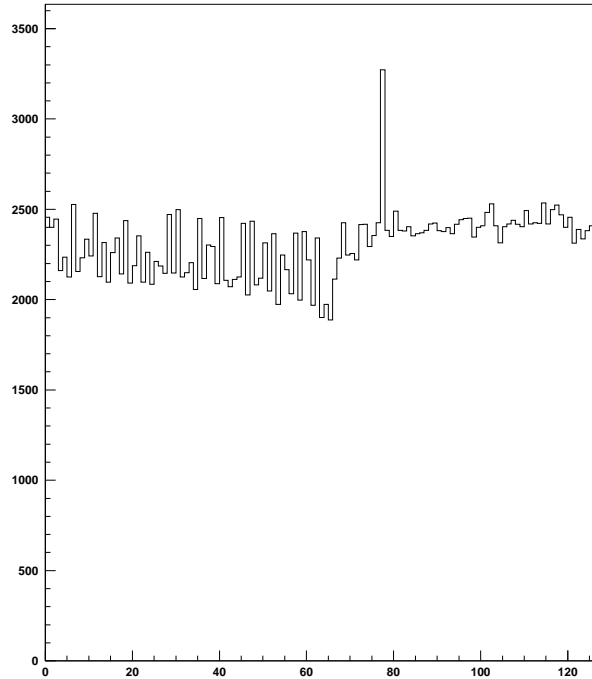
FIG. 10: This is the same picture as above, zooming in to the first chip-carrier of the second chain.

chip-carrier at a time. Then repeat for the other half of the channels and then do that for seven different pulse heights - a total of 14 runs. This worked, and although it would take longer than originally anticipated if Big Cal was to be performed as a single run, it was still well within the practical time limits. Meanwhile, I was preparing code in SUEZ that would be used to analyze the data once Big Cal was running. The final result of this software would be to calculate gain functions for every channel in the detector.

Once Big Cal was working on the teststand we were ready to move to the detector itself. Here we quickly learned that the procedure would have to be split up even further. Each run would now consist of a single pulse being sent to 32 channels instead of 64. This would double the number of runs and it would mean that the entire process would take a couple of hours. This was still a reasonable feat, so we moved forward. Unfortunately, after taking approximately 50 events the Data Acquisition System started crashing. Being under very tight time constraints the decision was to leave Big Cal to be completed when there was an expert available to assist in getting the Data Acquisition System to perform as it should. Without somebody around who knew the subtleties between the teststand and the main system we were playing a guessing game and ultimately the time could have been used more efficiently.

IV.   PULSE HEIGHT DISTRIBUTIONS OF CHERENKOV PHOTONS

My final survey into the electronics system of the RICH involved studying pulse height distributions of photons produced in a data-taking run for every window in the RICH. A window is simply a geometrical location on the detector cylinder and it is classified in the following way: the surface area of the cylinder is divided into 30 "chambers" or "sectors" along the longitudinal direction. Each one of these sectors is then split into eight windows. Fig. 11 is for Sector 24 Window 4 and it shows a typical distribution of signals that are thought to be produced by Cherenkov photons. There are 240 of such graphs (one for each window) that were generated by already existing code. My job was to fit each of these distributions to an exponential function and study their "decay" factor. In other words, I was interested in the value of γ in $e^{-1/\gamma}$.

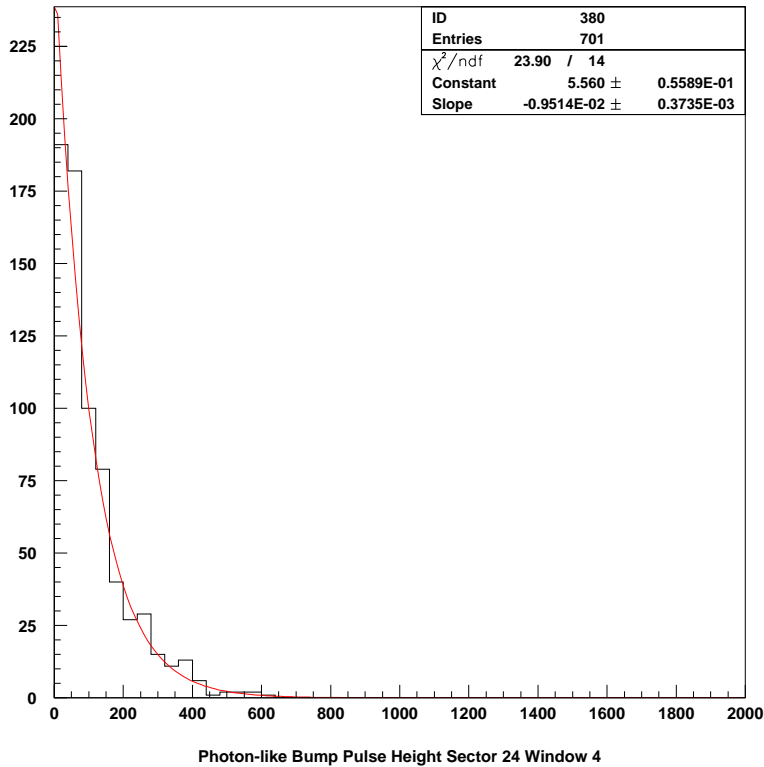| ID	380
Entries	701
χ^2/ndf	23.90 / 14
Constant	5.560 ± 0.5589E-01
Slope	-0.9514E-02 ± 0.3735E-03

Photon-like Bump Pulse Height Sector 24 Window 4

FIG. 11: A typical distribution of pulse heights thought to be caused by Cherenkov photons, fitted to the function $e^{-1/\gamma}$.

The value of γ, or the chamber gain of each window was set to a specific value when the RICH detector was first installed. However, since that time these values have not been monitored. If some windows exhibit values of chamber gain that are not optimal then the voltages can be adjusted in those areas of the detector to get the gain values back to where they should be. Fig. 12 shows the distribution of these values for the entire detector. We see that most of the windows have gain values just where they should be (within the Gaussian curve). There are several windows, however, that have values of gain that are either too high or too low. The plot is divided into five sections which correspond to the color codings

used in the next graph. Fig. 13 is the geometrical distribution of these gain values. White boxes correspond to windows that have gain values that are lower than what we would like. Red boxes correspond to windows that have gain values that are too high. Knowing exactly where these windows are located, we could now perform the necessary adjustments.
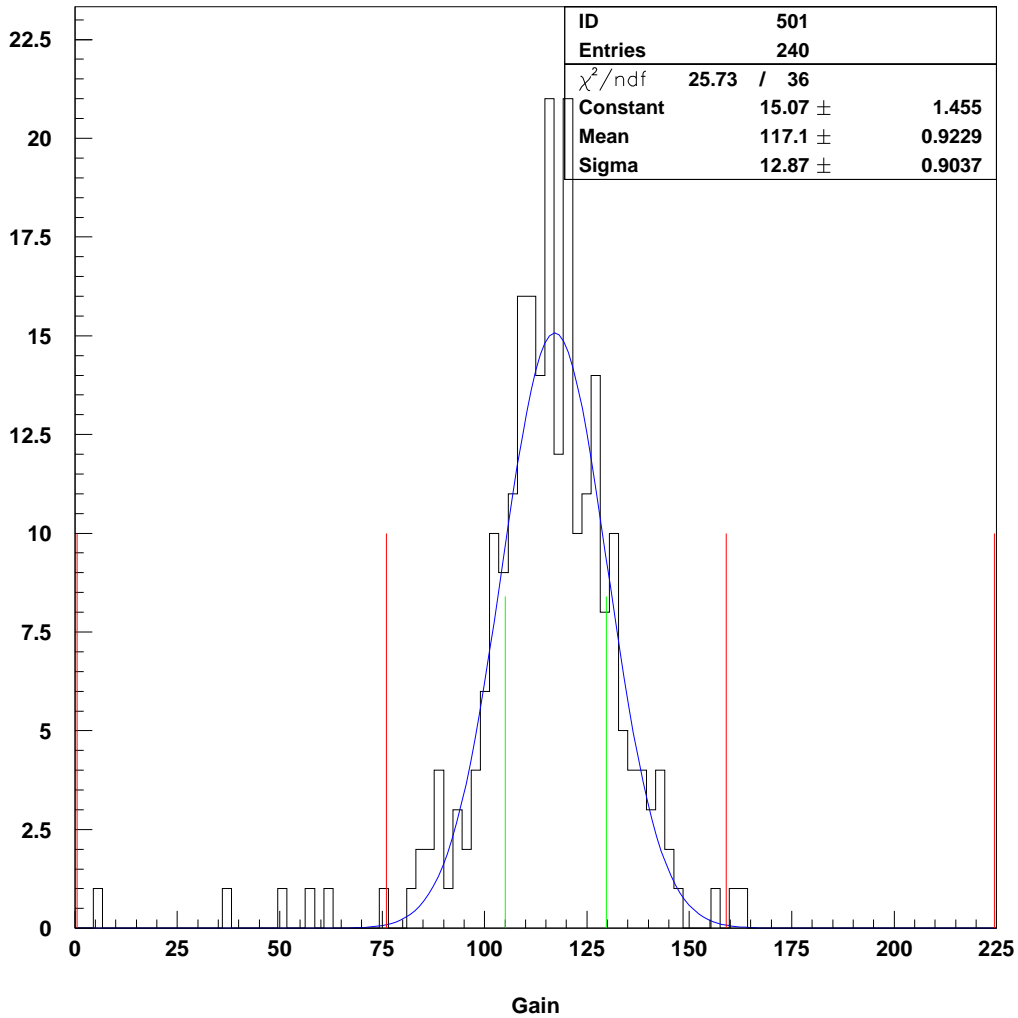

ID		501	
Entries		240	
χ^2/ndf	25.73	/ 36	
Constant		15.07 $\pm$	1.455
Mean		117.1 $\pm$	0.9229
Sigma		12.87 $\pm$	0.9037

FIG. 12: This is the distribution of the values of chamber gain in each window. The graph is divided into five sections which correspond to the the five color codings in the next plot.

V.   CONCLUSIONS

Based on statistical studies into the nature of noise levels and flat chips over the last three years, there is some indication that there is a correlation between these two problems. We now also have a better understanding of how the situation has been developing. Although the numbers of both flat chips and noisy channels have been steadily increasing, over 95%
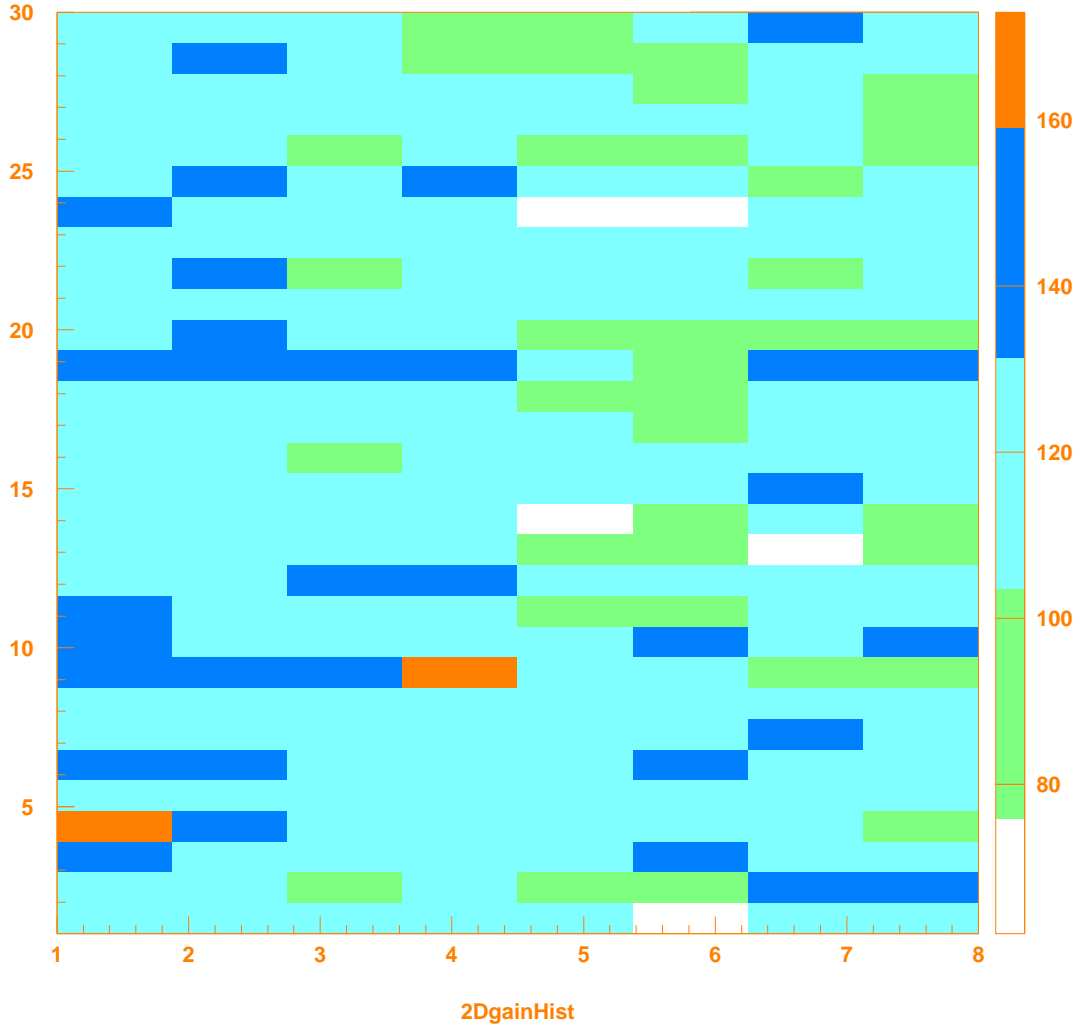
FIG. 13: This is a 2-dimensional plot of the gain values throughout the RICH. White boxes correspond to windows with low gain, red boxes to windows with high gain.

of the electronics in the detector is operating well. The new clues found this summer will be helpful in correcting the problems of noise and flatness in the future. Big Calibration mode will be one of the tools used to further study the malfunctioning components of the electronics system. Analysis code is prepared to generate the gain functions of individual channels, and Big Cal is expected to be completed in the next few weeks. Finally, photon-like pulse height distributions were surveyed for each window in the detector. A small number of windows were found to have chamber gains that are unfavorable and the proper adjustments are planned.

VI. ACKNOWLEDGMENTS

---

[1] More information about the Cherenkov effect can be found at:
    http://physics.syr.edu/research/elementary_particles/experimental/rich.html
[2] More information about CLEO III can be found at:
    http://www.lns.cornell.edu/public/CLEO .
[3] http://physics.syr.edu/research/elementary_particles/experimental/rich_elec_doc.html .
[4] A. Deisher, *Optimization of RICH Electronics*, August 2001. See:
    http://www.lns.cornell.edu/public/reu .
[5] Further information concerning latch-up can be found at:
    http://www.thermokeytek.com/cr/test_methods.htm .